Received: 17 January 2018 | Revised: 25 March 2018 | Accepted: 4 April 2018

DOI: 10.1002/mmce.21402

RESEARCH ARTICLE

WILEY INTERNATIONAL JOURNAL OF RF AND MICROWAVE COMPUTER-AIDED ENGINEERING

A-shaped wideband dielectric resonator antenna for wireless communication systems and its MIMO implementation

Abhishek Sharma | **Anirban Sarkar** | **Animesh Biswas** | **M. Jaleel Akhtar**

Department of Electrical Engineering, Indian Institute of Technology Kanpur, Kanpur, India

Correspondence
Abhishek Sharma, Department of Electrical Engineering, Indian Institute of Technology Kanpur, Kanpur, India.
Email: abhisheksharma.rf@gmail.com

Abstract

In this article, a new A-shaped dielectric resonator antenna (DRA) excited by a conformal strip is proposed for wideband applications. The wide bandwidth is achieved by combining two adjacent modes that is, TM_{101} and TM_{103}. The experimental results demonstrate that the proposed DRA offers an impedance bandwidth (for $S11 \leq -10$ dB) of 59.7% (3.24-6.0 GHz), covering IEEE 802.11 and U-NII bands. The antenna provides a fairly stable radiation pattern with the gain ranging from 5.29 to 7 dBi across the operating bandwidth. A dual-element multiple-input multiple-output (MIMO) system is also realized using the proposed wideband DRA. The impedance bandwidth of the dual-element MIMO antenna is 59.2% and 60.9% for *Port1* and *Port2,* respectively and the isolation between the ports is better than 20 dB across the bandwidth. For *Port1*, the gain of the MIMO antenna ranging from 6.03 to 7.45 dBi is obtained across the bandwidth. Furthermore, the diversity performance of the MIMO antenna is found to be good with envelope correlation coefficient below 0.003 over the operating band. The proposed antenna could be the potential candidate for worldwide interoperability for microwave access (WiMAX), wireless local area network (WLAN) and lower European UWB frequency band (3.4-5.0 GHz) applications.

KEYWORDS

MIMO antenna, mode merging, Wideband DRA, WLAN, WiMAX

1 | INTRODUCTION

Dielectric resonator antennas (DRAs) have gained widespread attention in wireless communication systems due to their attractive features such as high radiation efficiency (due to lack of surface wave and conductor losses), relatively wide bandwidth, and light weight.[1] Moreover, its size and bandwidth can be controlled by the dielectric constant of the material used to design the DRA. Being a volumetric radiator (3D structure), it offer more design flexibility and versatility than the conventional planar antennas. However, for the single-mode DRA the impedance bandwidth is typically 10%, which may not be sufficient for some broadband wireless communication systems.

The bandwidth enhancement of DRA has been the vital topic of study over the years and different techniques have been proposed to widen the bandwidth of DRAs. For instance in Ref. 2, stacking of multi-permittivity DRs has been used to enhance the bandwidth of DRA and by utilizing three layers, 38% of impedance bandwidth has been obtained. The mode merging technique has been utilized for bandwidth enhancement in Ref. 3. The specialized feeding mechanism such as tall microstrip line[4] also helps to improve the impedance bandwidth and using this technique the impedance bandwidth of 25% has been achieved. In Ref. 5, two adjacent DRs located asymmetrical with respect to the center of coupling aperture have been utilized to achieve the broadband characteristics. In Ref. 6, a dual-segmented DRA excited by S-shaped aperture has been reported with the impedance bandwidth of 41%. The DR loaded with parasitic strips and patches has been used in Ref. 7 to enhance the bandwidth of the DRA. A probe fed uniaxial anisotropic

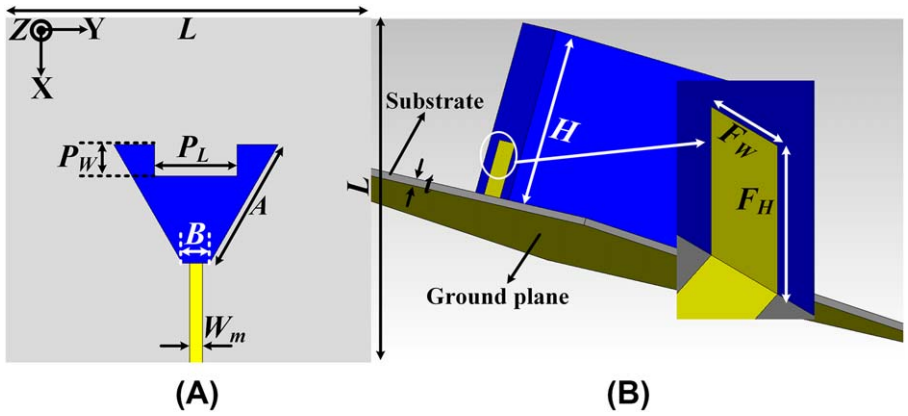

FIGURE 1 Geometry of proposed wideband DRA. A, Top view, B, 3D view

rectangular DRA having the impedance bandwidth of 19.4% has been reported in Ref. 8. Tailoring the shape of DR in the efficient manner also enhances the impedance bandwidth and several DRAs with tailored geometries such as bow-tie,[9] apollaian gasket,[10] dumbbell-shaped,[11] inverted umbrella shaped,[12] mushroom-shaped,[13] H-shaped[14] and E-shaped[15] have been reported for the wideband operations. The designs reported in Refs. 13 and 14 required a customized inverted trapezoidal patch feed in order to get the better matching over the specified frequency band. It has also been observed in Refs. 14 and 15 that the radiation patterns were not symmetrical and have some deformation at the higher frequency. All the above reported designs have either employed rectangular or cylindrical shaped DRAs and over the last few decades these geometries have been investigated widely. However, the DRAs with triangular cross section have not been explored much. The advantage of using triangular DRA is that it offers a smaller area as compared to the rectangular DRA for same height and permittivity when operating at the same resonant frequency.[1] However, using the triangular DRA the maximum impedance bandwidth of 47.4% has been achieved in Ref. 16.

In this article, a new and novel wideband A-shaped DRA excited by a simple rectangular conformal strip connected to a 50Ω microstrip line is proposed and investigated for wideband operation. This non-conventional shape of the DRA is derived from the structural modification of the equilateral triangular DRA. The wide bandwidth is achieved by merging the two adjacent modes viz. TM_{101} and TM_{103}. In addition to this, the perturbation in the structure also helps to improve the bandwidth by reducing the Q-factor. The proposed antenna offer an impedance bandwidth of 60% which is more than the earlier reported work based on the triangular DRAs.[16–21]

The multiple-input multiple-output (MIMO) technology has emerged as a new paradigm for modern wireless communication systems and is used in most of the wireless standards. The use of multiple radiators at both the transmitting and receiving ends in MIMO systems improves the link reliability and enhances the channel capacity without additional power requirement.[22] The attractive features of the DRA and the ability to excite different modes having distinct radiation characteristics make the DRA a potential candidate for diversity and MIMO applications. Therefore, DRAs are now

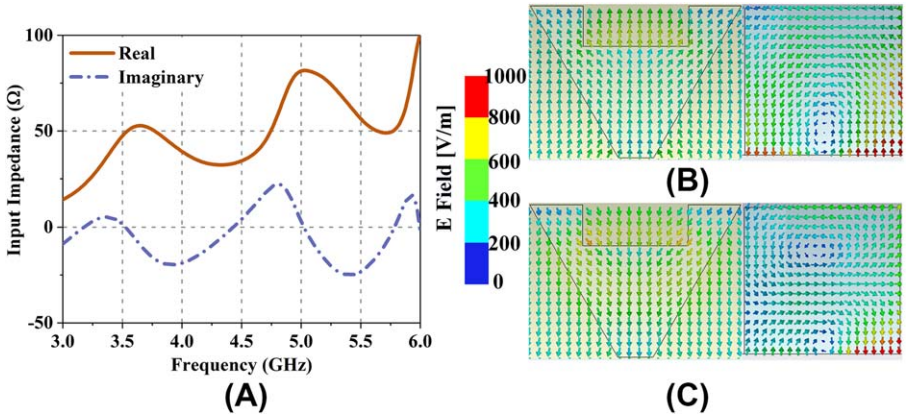

FIGURE 2 A, Simulated input impedance plot. B, Electric field distribution at 3.65 GHz. C, Electric field distribution at 5.04 GHz

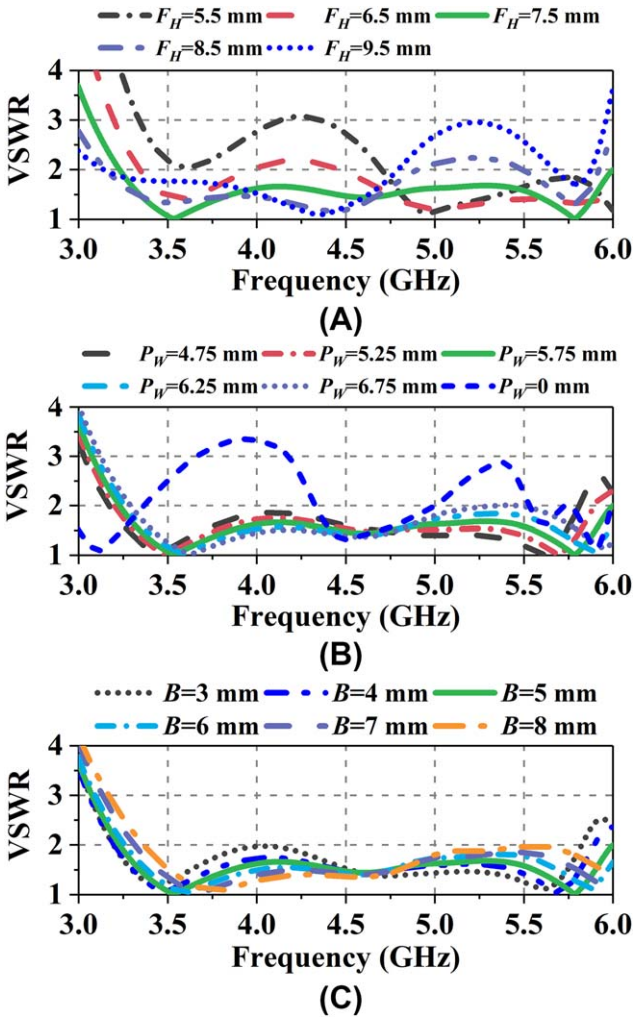

FIGURE 3 Simulated VSWR for different values of A, feed length F_H. B, Notch depth P_W. C, Chamfered tip length B

being utilized to design MIMO systems covering both microwave and millimeter wave frequency bands.[13,23–28] In this article, the applicability of the proposed wideband antenna for MIMO system is also demonstrated. For this, a dual-element MIMO antenna offering polarization diversity is implemented and its diversity performance is studied in terms of envelope correlation coefficient and total active reflection coefficient.

2 | SINGLE ELEMENT: WIDEBAND DRA

The geometry of proposed wideband A-shaped DRA is shown in Figure 1. The DR is placed on a low permittivity substrate (RT/Duroid 5880, ε_{rs} = 2.2, tanδ = 0.0009) of dimension 70 × 70 mm ($1.07\lambda_0 \times 1.07\lambda_0$, λ_0 being calculated at center frequency).

The material used to design DR is Rogers RT/Duroid 6010 of relative permittivity 10.2 and loss tangent 0.0023. In order to excite the DRA, a conformal rectangular strip of length F_H and width F_W is used.

2.1 | Modes and field distribution

Figure 2A shows the input impedance behavior of the proposed wideband antenna. From the figure, it is observed that the two resonances exist at 3.65 and 5.04 GHz in the desired frequency band. In order to gain insight into the resonant modes at these two frequencies, the modal electric field distributions are portrayed in Figure 2B,C.

The electric field distribution at 3.65 GHz resembles the fundamental TM_{101} mode whereas at 5.04 GHz it corresponds to higher order TM_{103} mode. For the unperturbed case that is for the equilateral triangular DRA having side length 30 mm and height 20.32 mm, the theoretical resonant frequency[29] of the fundamental TM_{101} mode is 3.05 GHz and that of higher order TM_{103} mode is 4.65 GHz. Since, the proposed structure is the perturbed version of equilateral triangular DR, therefore, the resonant frequency of both the modes get shifted to the higher side because of reduction in the effective permittivity. This reduction in the effective

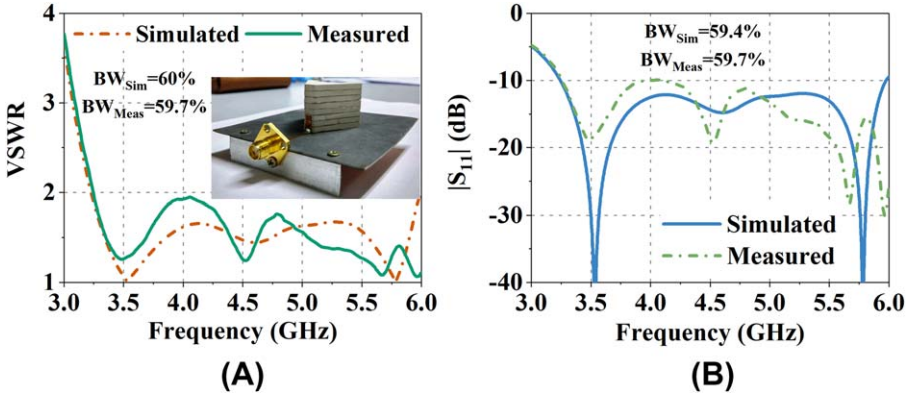

FIGURE 4 Simulated and measured response of the proposed wideband DRA. A, VSWR. B, Reflection coefficient

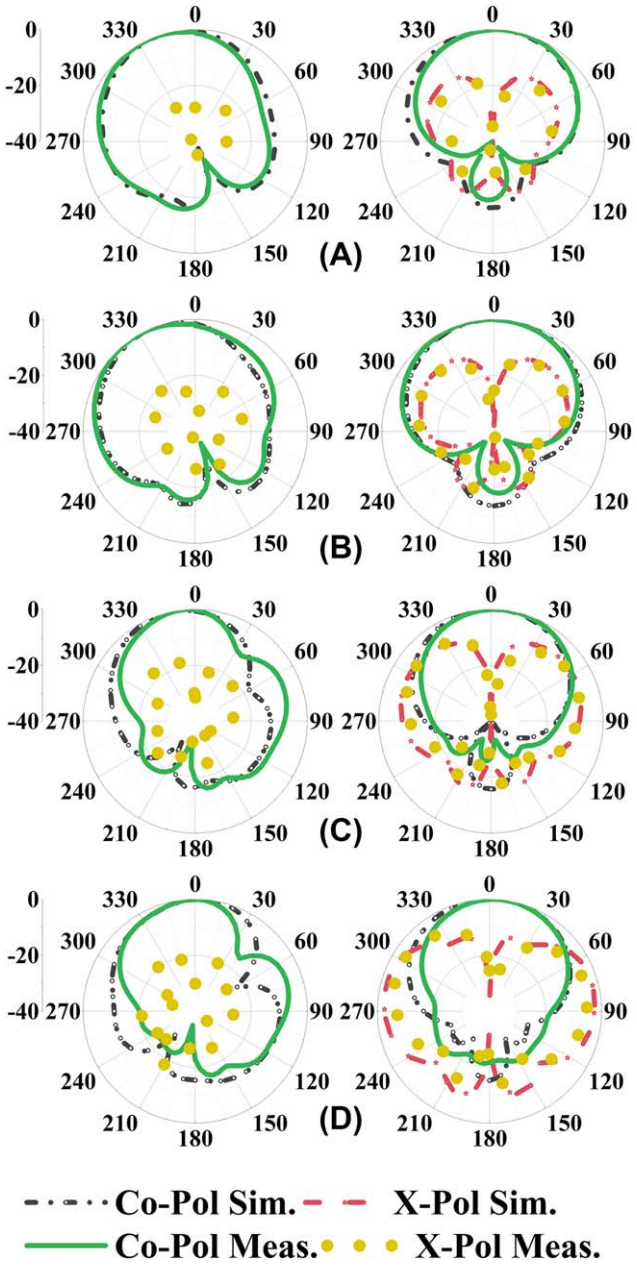

FIGURE 5 Simulated and measured normalized radiation pattern at A, 3.6 GHz, B, 4.25 GHz, C, 5 GHz, and D, 5.6 GHz (left side: *xz*-plane and right side: *yz*-plane)

permittivity also helps to improve the bandwidth by lowering down the quality factor ($Q \propto (\varepsilon_{eff})^P$ with $P \geq 1$).[30]

2.2 | Parametric analysis

Figure 3A shows the simulated response of the proposed antenna for different values of feed length F_H and the pronounce effect on impedance matching is observed. It is observed form the figure that the feed length, $F_H = 7.5$ mm provides good matching throughout the desired frequency band.

The effect of P_W on the bandwidth of the proposed antenna is depicted in Figure 3B. On increasing the value of P_W, the effective permittivity decreases which in turn reduces Q-factor and enhances the impedance bandwidth. Due to the reduction in effective permittivity, frequency band start shifting slightly to the higher side and the impedance matching starts deteriorating. Therefore, for the best bandwidth in the desired frequency band, the value of P_W is chosen as 5.75 mm.

The effect of B on the antenna bandwidth (refer Figure 3C) can be explained in the same way as above. The increase in the value of B also degrades the impedance matching on the higher side of frequency band. Thus, for the maximum bandwidth in the desired frequency band and at the same time maintaining the impedance matching, the value of B is chosen as 5 mm.

2.3 | Experimental results

The dimensions of the proposed wideband DRA are: $A = 25$ mm, $H = 20.32$ mm, $B = 5$ mm, $P_W = 5.75$ mm, $P_L = 15$ mm, $t = 0.787$ mm, $F_H = 7.5$ mm, and $F_W = 2.4$ mm. Figure 4 shows the VSWR and reflection coefficient of the proposed wideband DRA.

For $S_{11} \leq -10$ dB, the simulated and measured impedance bandwidth of the proposed antenna is 59.4% (3.24-5.98 GHz) and 59.7% (3.24-6 GHz), respectively. Figure 5 shows the comparison between the simulated and measured normalized radiation pattern of the proposed antenna.

The radiation pattern of the antenna is fairly stable throughout the bandwidth and the cross polarization level is below −20 dB along the zenith. Across the bandwidth, the simulated and measured gain of the proposed antenna varies from 5.05–7.22 dBi to 5.29-7 dBi, respectively as shown in Figure 6A.

The simulated efficiency of the proposed antenna is greater than 89% throughout the operating band. The slight discrepancy between the simulated and measured results is owing to the fabrication tolerances, air gap between DR and the low permittivity substrate.

Table 1 shows the comparison of proposed antenna with the some recent work on wideband DRAs.

3 | DUAL ELEMENT: MIMO WIDEBAND DRA

3.1 | Impedance performance

Figure 7A depicts the schematic of dual-element MIMO DRA which offer polarization diversity.

The isolation performance of the MIMO antenna for different values inter-element spacing S is shown in Figure 7B. From, the figure it is observed that on increasing the value of

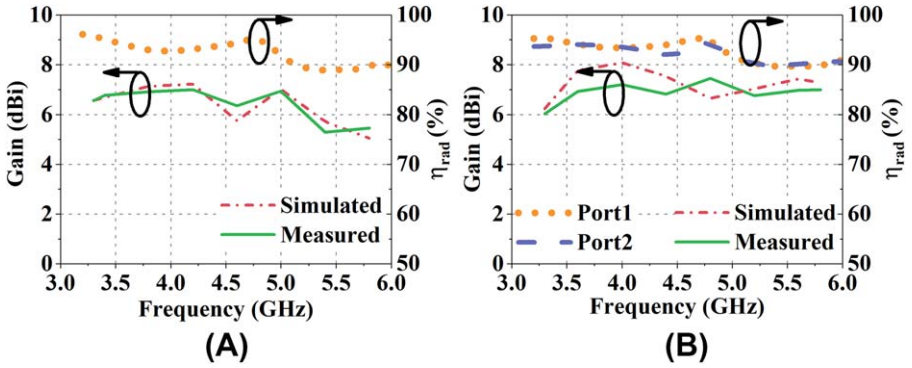

FIGURE 6 A Simulated and measured gain of the proposed wideband DRA. B, Simulated and measured gain of the MIMO antenna at *Port1*

S, the port-to-port isolation gets better. For the present design, the value of *S* is chosen as 21.4 mm as it gives the isolation better than 20 dB over the bandwidth. A comparison between the simulated and measured response of the MIMO antenna is depicted in Figure 8A,B.

For $S_{11} \leq -10$ dB, the simulated impedance bandwidth is 58.5% (3.25-5.94 GHz) and 60.3% (3.21-5.98 GHz) for *Port1* and *Port2*, respectively and the corresponding measured values are 59.2% (3.26-6 GHz) and 60.9% (3.20-6 GHz). Both the simulated and measured port-to-port isolation is better than 20 dB throughout the operating band as shown in Figure 8C.

3.2 | Radiation performance

Figure 9 shows the simulated and measured normalized radiation pattern of the antenna element *DR1* (*Port1*) with *Port2* terminated into the matched load.

The radiation pattern is fairly stable and the difference between the co-polarized and cross-polarized field is nearly 15 dB in simulation and 12 dB in measurement. Across the operating frequency band, the simulated and measured gain of the MIMO antenna varies in the range of 6.23-8.08 dBi to 6.03–7.45 dBi, respectively as shown in Figure 6B. It should be noted that the antenna element *DR2* radiates in similar manner when *Port1* is terminated into matched load and therefore, their radiation pattern plots are not shown for brevity.

3.3 | MIMO performance metrics

The envelope is the primary performance metric to evaluate the performance of MIMO antenna system. ECC considers the far field property of the MIMO antenna system and its value can be computed as[13]

TABLE 1 Comparison with other related wideband DRAs

Ref.	DRA type	Feeding	Coverage band (GHz)	Bandwidth (%)	Peak gain (dBi)	Antenna size (λ_0^3)
[5]	Cylindrical	Aperture coupling	9.62-12.9	29	6.34-7.22	1.12 × 0.94 × 0.34
[6]	Cylindrical	S-shaped aperture	7.8–11.85	41	6	0.82 × 0.98 × 0.30
[8]	Rectangular	Probe	3.40-4.13	19.4	8.1	1.25 × 1.25 × 0.21
[10]	Hemispherical	Probe	3.50-5.10	37	8.7	1.43 × 1.43 × 0.36
[11]	Dumbbell shaped	Probe	4.11-6.69	47.8	NA	NA
[12]	Inverted umbrella	Microstrip line	5–6.67	28	2.2–5.2	0.97 × 0.97 × 0.1
[13]	Mushroom shaped	Trapezoidal patch	4.56-9.96	74	NA	1.5 × 1.5 × 0.39
[15]	E-shaped	Strip	6.00–10.20	51.85	4.5–8.1	1.35 × 1.35 × 0.14
[16]	Isosceles triangular	Probe	4.33-7.02	47.4	NA	2.6 × 2.6 × 0.36
Proposed Antenna	**A-shaped**	**Strip**	**3.24-6.00**	**59.7**	**5.29-7**	**1.07 × 1.07 × 0.31**

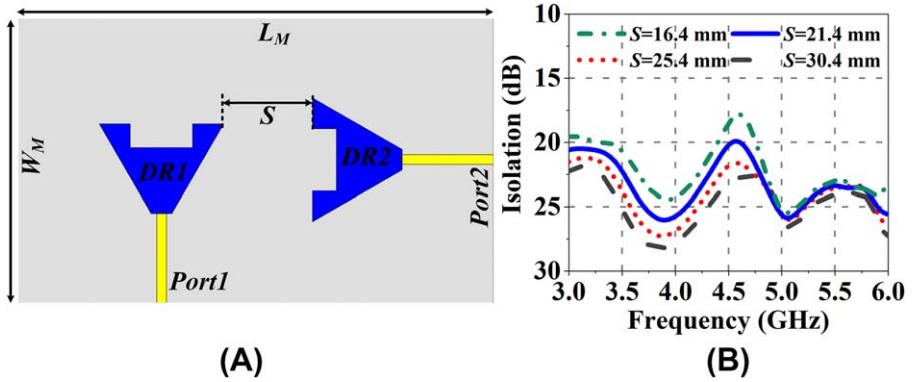

FIGURE 7 A, Geometry of dual-element MIMO DRA (geometrical parameters: $L_M = 115$, $W_M = 70$, S = 21.4 (all dimensions are in mm). B, Isolation for different values of inter-element spacing S

$$\rho_{eij} = \left| \frac{\iint_{4\pi} \text{XPR}\ E_{\theta i}(\Omega)E^*_{\theta j}(\Omega)P_\theta(\Omega) + E_{\phi i}(\Omega)E^*_{\phi j}(\Omega)P_\phi(\Omega)d\Omega}{\sqrt{\iint_{4\pi} \text{XPR}\ G_{\theta i}(\Omega)P_\theta(\Omega) + G_{\phi i}(\Omega)P_\phi(\Omega)d\Omega \iint_{4\pi} \text{XPR}\ G_{\theta j}(\Omega)P_\theta(\Omega) + G_{\phi j}(\Omega)P_\phi(\Omega)d\Omega}} \right|^2 \quad (1)$$

where $E_i(\Omega)$ is the 3D complex field pattern of antenna element i,$\Omega$is the solid angle,$P_\theta(\Omega)$ and $P_\phi(\Omega)$ are the angular density function, $G_\theta(\Omega) = E_\theta(\Omega)E_\theta(\Omega)^*$, XPR denotes the cross polarization power ratio and $\{\cdot\}^*$denotes the complex conjugate. The complex far field pattern for each element is extracted from CST to compute the ECC using Equation 1. For isotropic and uniform propagation scenario (XPR = 1 and $P_\theta(\Omega) = P_\phi(\Omega) = 1/4\pi$),[22] the variation of the ECC is shown in Figure 10A and it is observed that its value is below 0.003 across the operating bandwidth. The ECC of the proposed MIMO antenna lies within the acceptable limit (ECC < 0.5), indicating effective diversity performance.

In order to characterize the bandwidth and radiation performance of the multiport antenna, total active reflection

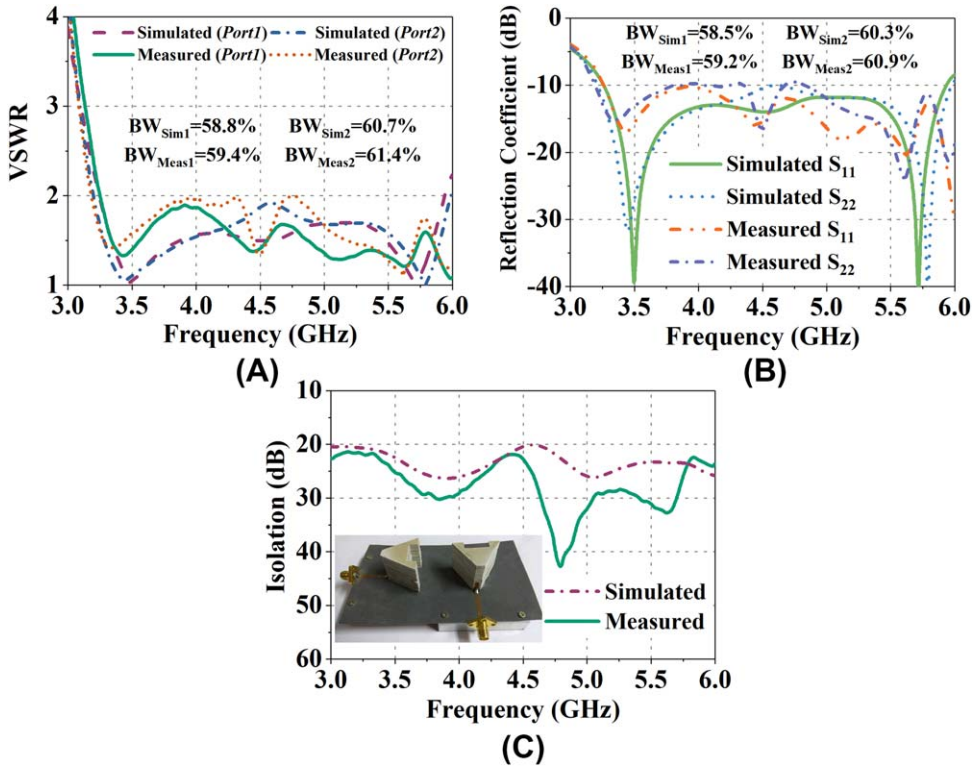

FIGURE 8 Simulated and measured response of the MIMO antenna. A, VSWR. B, Reflection coefficient. C, Isolation

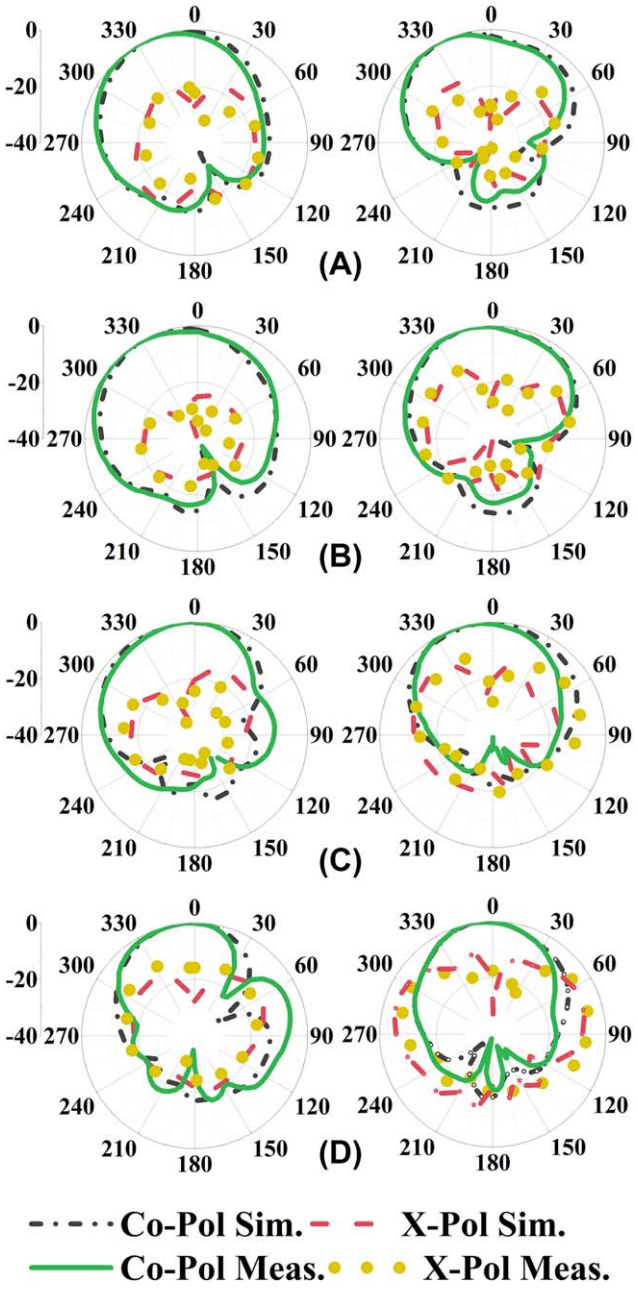

FIGURE 9 Simulated and measured normalized radiation pattern of MIMO system for antenna element *DR1* at A, 3.6 GHz, B, 4.25 GHz, C, 5 GHz, and D, 5.6 GHz (left side: *xz*-plane and right side: *yz*-plane)

coefficient (TARC) is evaluated. It accounts the mutual coupling between the elements and random signal combinations between the ports. TARC for N-port antenna system is defined as the ratio of square root of total reflected power to the square root of total incident power[22]

$$\Gamma_a^t = \frac{\sqrt{\sum_{i=1}^{N} |b_i|^2}}{\sqrt{\sum_{i=1}^{N} |a_i|^2}} \tag{2}$$

where a_i is the incident signal, b_i is the reflected signal and both are related with scattering parameters as $\mathbf{b} = [S]$

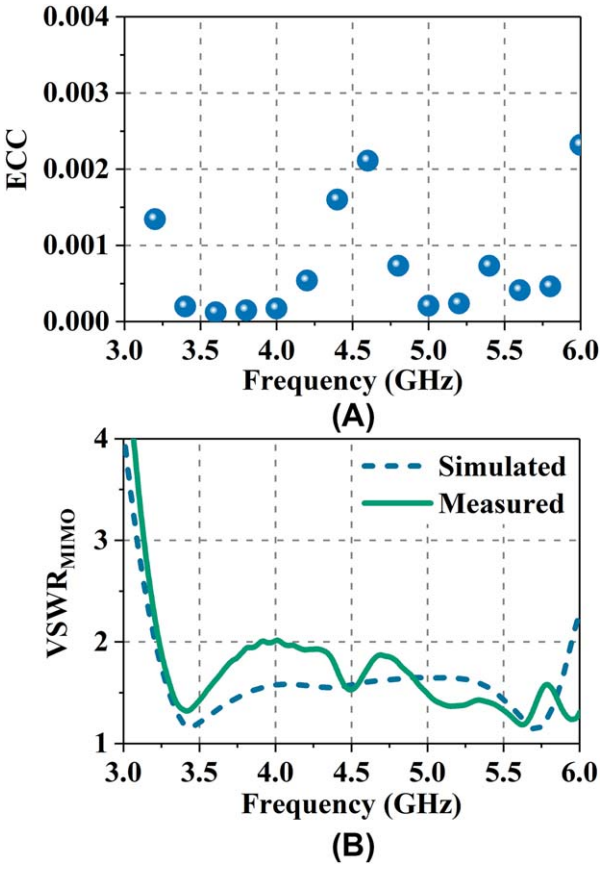

FIGURE 10 Diversity performance metrics. A, Envelope correlation coefficient. B, $VSWR_{MIMO}$

a. Using Equation (2), VSWR for MIMO system can be defined as[13]

$$VSWR_{MIMO} = \frac{1+\Gamma_a^t}{1-\Gamma_a^t} \tag{3}$$

The simulated and measured variation of $VSWR_{MIMO}$ is depicted in Figure 10B. From the figure, it is inferred that VSWR curve retain the original behavior of a single antenna characteristics with the slight change in bandwidth.

4 | CONCLUSION

A new dielectric resonator antenna in the form of A-shape and excited by a conformal rectangular strip has been proposed and investigated for wideband applications. This A-shaped DRA achieves a wide impedance bandwidth of 59.7% (3.24-6 GHz), covering IEEE 802.11 and U-NII frequency bands. Furthermore, the proposed antenna offers a stable radiation broadside radiation with the gain ranging from 5.29 to 7 dBi across the bandwidth. The proposed wideband radiator is then utilized to implement a dual-element MIMO system. The MIMO antenna exhibits the impedance bandwidth of 59.2% and 60.9% for *Port1* and *Port2,* respectively and the isolation better than 20 dB has

been achieved throughout the bandwidth. The gain of the MIMO antenna for *Port1* varies from 6.03 to 7.45 dBi over the working frequency band. The diversity performance of the antenna has been found good with the envelope correlation coefficient better than 0.003 throughout the bandwidth. The proposed antenna finds application in worldwide interoperability for microwave access (WiMAX), wireless local area network (WLAN) and lower European UWB frequency band (3.4–5.0 GHz).

ORCID

Abhishek Sharma http://orcid.org/0000-0001-8026-9752
Anirban Sarkar http://orcid.org/0000-0003-2592-8967

REFERENCES

[1] Petosa A. *Dielectric Resonator Antenna Handbook*. Boston: Artech House.

[2] Chaudhary RK, Srivastava KV, Biswas A. A practical approach: Design of wideband cylindrical dielectric resonator antenna with permittivity variation in axial direction and its fabrication using microwave laminates. *Microw Optic Technol Lett.* **2013**;55(10): 2282–2288.

[3] Fang XS, Leung KW. Designs of single-, dual-, wide-band rectangular dielectric resonator antennas. *IEEE Trans Antenna Propag.* **2011**;59(6):2409–2414.

[4] Klymyshyn DM, Shafai L, Rashidian A. Tall microstrip transmission lines for dielectric resonator antenna applications. *IET Microw Antenna Propag.* **2014**;8(2):112–124.

[5] Majeed AH, Abdullah AS, Elmegri F, et. al. Aperture-coupled asymmetric dielectric resonators antenna for wideband applications. *IEEE Antenna Wireless Propag Lett.* **2014**;13:927–931.,

[6] Elmegri F, Abdullah AS, Abd-Alhameed RA, et. al. Dual-segment S-shaped aperture-coupled cylindrical dielectric resonator antenna for X-band applications. *IET Microw Antenna Propag.* **2015**;9(15):1673–1682.,

[7] Kamran Saleem M, Alkanhal MAS, Sheta AF. Switched beam dielectric resonator antenna array with six reconfigurable radiation patterns. *Int J RF Microw Comput Aided Eng.* **2016**;26(6): 519–530.

[8] Fakhte S, Oraizi H. Compact uniaxial anisotropic dielectric resonator antenna operating at higher order radiating mode. *IET Electron Lett.* **2016**;64:2914–2922.

[9] Thame LZ, Wu Z. Broadband bowtie dielectric resonator antenna. *IEEE Trans Antenna Propag.* **2010**;58:3707–3710.

[10] Mukherjee B, Patel P, Mukherjee J. Hemispherical dielectric resonator antenna based on apollonian gasket of circles: A fractal approach. *IEEE Trans Antenna Propag.* **2014**;62(1):40–47.

[11] Chaudhary RK, Srivastava KV, Biswas A. A broadband dumbbell-shaped dielectric resonator antenna. *Microw Opt Technol Lett.* **2014**;56(12):2944–2947.

[12] Vinodha E, Raghavan S. A broadband inverted umbrella shaped cylindrical dielectric resonator antenna for "WLAN" and "C" band applications. *Int JRF Microw Comput Aided Eng.* **2017**;27 (6):e21100–e21107.

[13] Sharma A, Biswas A. Wideband multiple-input multiple-output dielectric resonator antenna. *IET Microw Antenna Propag.* **2017**; 11(4):496–502.

[14] Liang XL, Denidni TA. H-shaped dielectric resonator antenna for wideband applications. *IEEE Antenna Wireless Propag Lett.* **2008**;7:163–166.

[15] Gupta RD, Parihar MS. Investigation of an asymmetrical E-shaped dielectric resonator antenna with wideband characteristics. *IET Microw Antenna Propag.* **2016**;10(12):1292–1297.

[16] Maity S, Gupta B. Experimental investigations on wideband triangular dielectric resonator antenna. *IEEE Trans Antenna Propag.* **2016**;64(12):5483–5486.

[17] Lo HY, Leung KW. Excitation of low-profile equilateral triangular dielectric resonator antenna using a conducting conformal strip. *Microw Opt Technol Lett.* **2001**;29(5):317–319.

[18] Kishk AA. A triangular dielectric resonator antenna excited by a coaxial probe. *Microw Opt Technol Lett.* **2001**;30(5):340–341.

[19] Leung KW, Chow KM, Luk KM. Low-profile high-permittivity dielectric resonator antenna excited by a disk loaded coaxial aperture. *IEEE Antenna Wireless Propag Lett.* **2003**;2:212–214.

[20] Kishk AA. Wideband truncated tetrahedron dielectric resonator antenna excited by a coaxial probe. *IEEE Trans Antenna Propag.* **2003**;51(10):2913–2917.

[21] Denidni TA, Rao Q, Sebak AR. Broadband L-shaped dielectric resonator antenna. *IEEE Antenna Wireless Propag Lett.* **2005**;4: 453–454.

[22] Sharawi MS. *Printed MIMO Antenna Engineering*. Boston: Artech House.

[23] Sun YX, Leung KW. Dual-band and wideband dual-polarized cylindrical dielectric resonator antennas. *IEEE Antenna Wireless Propag Lett.* **2013**;12:384–387.

[24] Fang XS, Leung KW, Luk KM. Theory and experiment of three-port polarization-diversity cylindrical dielectric resonator antenna. *IEEE Trans Antenna Propag.* **2014**;62(10):4945–4951.

[25] Roslan SF, Kamarudin MR, Khalily M, et. al. An MIMO rectangular dielectric resonator antenna for 4G applications. *IEEE Antenna Wireless Propag Lett.* **2014**;13:321–324.,

[26] Sharma A, Sarkar A, Biswas A, Sloan R, Hu Z. A polarization diversity substrate integrated waveguide fed rectangular dielectric resonator antenna in 2016 Asia-Pacific Microwave Conference (**2016**).

[27] Das G, Sharma A, Gangwar RK. Dual-port aperture coupled MIMO cylindrical dielectric resonator antenna with high isolation for WiMAX application. *Int J RF Microw Comput Aided Eng.* **2017**;27(7):e21107

[28] Sharawi MS, Podilchak SK, Hussain MT, et. al. Dielectric resonator based MIMO antenna system enabling millimeter-wave mobile devices. *IET Microw Antenna Propag.* **2017**;11(2):287–293.,

[29] Maity S, Gupta B. Theoretical investigations on equilateral triangular dielectric resonator antenna. *IET Microw Antenna Propag.* **2017**;11(2):184–192.

[30] Patel P, Mukherjee B, Mukherjee J. A compact wideband rectangular dielectric resonator antenna using perforations and edge grounding. *IEEE Antenna Wireless Propag Lett.* **2015**;14:490–493.

AUTHOR BIOGRAPHIES

ABHISHEK SHARMA received the B Tech degree in Electronics and Communication Engineering from Shri Mata Vaishno Devi University, Jammu, India, in 2010 and M Tech degree in RF and Microwave Engineering from AIACTR, New Delhi, India, in 2013. Currently, he is pursuing the PhD degree from Indian Institute of Technology Kanpur, Kanpur, India. He has authored/co-authored 13 peer-reviewed journals and 18 international conference papers. His current research interests include dielectric resonator antennas, MIMO antennas and SIW based leaky wave antennas. He is a Graduate student member of IEEE and student member of European Microwave Association. Mr. Sharma has served as Treasurer and Chapter Chair of IEEE MTT-S Student Branch Chapter, IIT Kanpur, in 2015 and 2016, respectively.

ANIRBAN SARKAR received the B Tech degree in Electronics and Communication Engineering from Hooghly Engineering and Technology College, Kolkata, India, in 2011 and ME degree in Microwave Communication from Indian Institute of Engineering Science and Technology, Shibpur, India in 2013. Currently, he is pursuing the PhD degree from Indian Institute of Technology Kanpur, Kanpur, India. He has authored/co-authored 8 peer-reviewed journals and 10 international conference papers. His current research interests include SIW based circuits, leaky wave antennas, and diversity antennas. Mr. Sarkar is a student member of IEEE and has served as webmaster of IEEE APS Student Branch Chapter, IIT Kanpur. He currently holds the position of Vice-Chair in IEEE APS Student Branch Chapter, IIT Kanpur and secretary in IEEE MTT-S Student Branch Chapter, IIT Kanpur.

ANIMESH BISWAS received the M Tech. degree in microwave and radar engineering from the IIT Kharagpur, India, in 1982, and the PhD degree in electrical engineering from the IIT Delhi, New Delhi, India, in 1989. From 1989 to 1990, he was a Post-Doctoral Fellow with Oregon State University, where he was involved in characterizing multi-conductor lines in layered medium. He is currently a Professor with the Department of Electrical Engineering, IIT Kanpur, Kanpur, India. He has served as a technical consultant for M/S COMDEV Europe, and was involved in development of multimode DR filters and diplexers. His current research includes modeling of microwaves circuits, RF integrated circuits (RFICs), and numerical methods for solving electromagnetic problems. He has authored or co-authored over 195 papers in various peer-reviewed international journals and conference proceedings. Prof. Biswas is a Fellow of the Institution of Electronics and Telecommunication Engineers, India and senior member of IEEE, USA.

M. JALEEL AKHTAR received the PhD degree in electrical engineering from the Otto-von-Guericke University of Magdeburg, Magdeburg, Germany, in 2003. He was a Scientist with the CEERI, Pilani, India, from 1994 to 1997. From 2003 to 2009, he was a Post-Doctoral Research Scientist and a Project Leader with the Institute for Pulsed Power and Microwave Technology, Karlsruhe Institute of Technology, Karlsruhe, Germany. In 2009, he joined the Department of Electrical Engineering, IIT Kanpur, Kanpur, India, where he is currently an Associate Professor. He has authored two books, two book chapters, and has authored or co-authored over 200 papers in various peer-reviewed international journals and conference proceedings. He holds two patents on RF sensors for testing of solid and liquid sample, and one patent on nanomaterial integrated RF sensor for detection of harmful gases in the environment. His current research interests include microwave and THz imaging, microwave nondestructive testing, metamaterial inspired RF sensors, SIW based RF devices and sensors, RF energy harvesting, UWB antennas for imaging, and design of RF filters and components using the electromagnetic inverse scattering. Dr. Akhtar is a fellow of the Institution of Electronics and Telecommunication Engineers, New Delhi, India, and a Life Member of the Indian Physics Association and the Indo-French Technical Association.

How to cite this article: Sharma A, Sarkar A, Biswas A, Akhtar MJ. A-shaped wideband dielectric resonator antenna for wireless communication systems and its MIMO implementation. *Int J RF Microw Comput Aided Eng*. 2018;28:e21402. https://doi.org/10.1002/mmce.21402